Holo-GPC: Holographic Generalized Phase Contrast

Andrew Bañas[a], Jesper Glückstad[b],*

[a] *OptoRobotix ApS, DK-2000 Frederiksberg, Denmark*
[b] *DTU Fotonik, Dept. Photonics Engineering, Technical University of Denmark, Ørsted Plads 343, DK-2800 Kgs. Lyngby, Denmark*

ARTICLE INFO

ABSTRACT

Light shaping methods based on spatial phase-only modulation can be classified depending on whether they distribute multiple beams or shape the individual beams. Diffractive optics or holography can be classified as the former, as it spatially distributes a plurality of focal spots over a working volume. On the other hand, Generalized Phase Contrast (GPC) forms beams with well-defined lateral shapes and could be classified as the latter. To certain extents, GPC and holography can also perform both beam distribution and beam shaping. But despite the overlap in beam distribution and beam shaping, it is clear that one approach outperforms the other in one of these aspects. In this work, we introduce a hybrid of holography and GPC, coined Holo-GPC, which can efficiently control both the individual shape and the collective distribution of the resulting light beams. Hereby, Holo-GPC obtains the simplicity of GPC in forming well-defined speckle-free shapes that can be distributed over an extended 3D volume through holographic means. The combined strengths of the two photon-efficient phase-only light shaping modalities open new possibilities for contemporary laser sculpting applications.

1. Introduction

Laser beam shaping has paved the way for many studies and applications and can be considered as a key enabling tool. It has been applied to fields as diverse as microbiology, neuroscience [1,2], optical manipulation [3], materials processing and even consumer related areas such as entertainment. Hence, the continued exploration of traditional light shaping modalities and the development of new ones can be as important as the applications where they are supposed to be used.

So far, common light shaping techniques can be loosely classified based on whether they are utilized to distribute multiple beams in parallel or whether they shape the beams individually. Both the collective spatial distribution of the beams and the shape of the individual beams have relevant roles. In many research applications such as optical manipulation [3] or biophotonics [1,2], light has to be targeted to the dynamic distribution of the tissue or particles in the experiment. Other applications that emphasize the beam distribution include optical fractionation and parallel materials processing where a periodic array of beams is commonly utilized. In such applications, the actual shape of the beam being distributed is often ignored and it is enough that the typically Gaussian, Airy-disk or Sinc beam profile has the required size.

While a lot can be achieved with a simple focused beam, significantly more can be done by shaping these beams to something other than just a circular spot. There are situations where the illuminated objects are no longer"point-like" and greater control of the interaction between light and matter is required. Even if it is possible to scan a sharply focused spot over a shaped region of interest, this is not the same as having a spatially shaped single shot exposure. For example in STED microscopy [4], it is necessary to have a"donut" shaped light profile that suppresses fluorescence excitation except at the center of the donut. The amount of refraction, reflection or absorption in an optically manipulated particle will also vary throughout the particle's extent, depending on its structure [5] or composition which can also be engineered [6]. Moreover, in laser materials processing, it has been shown that tailored patterned beams can control the melt flow out and kerf [7]. Therefore, given more advanced applications, a typical center-weighted beam profile would no longer necessarily be the most suitable light distribution.

Hence, even though holography can address multiple sites in a sample in parallel, much more can be achieved if the shape of the light in these respective sites can be modified while maintaining the efficiency advantages of phase-only spatial modulation. Although it is possible to group multiple diffraction-limited holographic spots to collectively form a "shape", such aggregated spots are not likely to have the same phase and intensities so the resulting reconstruction would look noisy and speckled. This noise becomes a problem especially in non-linear optics applications where it would be further emphasized [2,8]. The random looking phase of such light distribution also makes

its propagation behavior less predictable. Instead of grouping focal spots, a workaround would be to shape the light around the individual focal spots themselves such that they obtain well-defined, noise- and speckle-free contiguous phase and intensity distributions. This can be achieved by Holo-GPC and will be explained and analyzed in the following.

1.1. Efficient and practical modification of the hologram read-out light

Just as the shape of generated individual output beams can be important, so is the shape of the light that is illuminating a hologram. Ultimately, the read-out illumination determines the amplitude and phase distribution of the point-spread function (PSF) at the output optical far-field plane. We are particularly interested in modifying the "spread function" of the output beams. As the typical illumination shape would have a tophat or a Gaussian distribution, the typical PSFs are either shaped as Airy-disks or Gaussians. The target output PSF can thus be changed by illuminating with an (inverse) far-field transformed beam shape. The challenge, therefore, is the efficient creation of an initial basis beam shape (typically using the Fourier transform) that will become the output's PSF.

It is well known that a Fourier transformed amplitude mask can be used to illuminate a hologram in order to get PSFs with the same amplitude pattern. Holo-GPC starts with a similarly looking phase mask that efficiently transmits the input light without absorbing photons. But unlike a straight-forward convolution, phase filtering is required to convert the phase mask into shaped PSFs at the output. As it relies on GPC's phase to intensity mapping, Holo-GPC also inherits GPC's efficiency advantage over amplitude masking and would in principle also have 3x brighter PSFs or over 90% of energy savings [9]. On the other hand, a similar amplitude mask would need to block up to ~70% of the input light to get a similar output.

As such, several light shaping methods have been proposed and used for hologram read-out. Perhaps the most familiar and most general is Bartlet's tandem configuration [10,11] which utilizes another hologram reconstruction to read-out a second hologram. Although Holo-GPC can be considered a special case of this, Holo-GPC's approach is much simpler as the computational or fabrication cost of the first hologram is replaced by a well-defined, easily fabricated, and generally reusable phase mask. In the usual tandem configuration, the first phase element which is a hologram generally bears no resemblance to the final output and would require re-calculation for different outputs which can make pre-fabricated phase elements impractical. Besides directly shaping the holographic beams, it is interesting to note that shaped GPC output has also been proposed for hologram read-out for a configuration similar to Bartlet's [12] or for efficient utilization of spatial light modulators [13].

2. Holo-GPC

To understand how Holo-GPC works, we first consider a standard GPC configuration and subsequently identify the modifications necessary to make multiple holographic copies of this GPC output. In a standard GPC setup (Fig. 1), the input phase mask is first optically Fourier transformed and the resulting distribution is focused on a phase contrast filter (PCF). An output intensity mapping of the input phase mask is generated from the interference of the imaged input with a so-called synthesized reference wave (SRW) that results from the low frequency components phase shifted by the PCF. For Gaussian illumination, this output can have an efficiency of up to ~84%.

Looking at the optics from the PCF plane, through the imaging lens, then to the output intensity (Figs. 1(d) to (g)), it can be seen that this is also a Fourier transforming setup. But unlike a typical hologram setup that uses Gaussian or tophat illumination, we instead have the optical Fourier transform of the input phase mask. This illumination typically resembles a Sinc function, or an Airy disk, but in general can be the Fourier transform of the desired PSF-shape with similar geometry as the input phase mask. Furthermore, GPC's PCF phase shift is correcting the central part, such that it matches the phase distribution of an ideal Sinc function or Airy disk [9]. Hence, through convolution, by placing a hologram phase on top of this PCF-shifted, Fourier-transformed phase mask, Holo-GPC can produce a beam distribution wherein each beam takes the form of the intensity mapped input illuminated phase mask as in Fig. 2.

As Holo-GPC operates by efficiently modifying the point spread function, the individual beams are identical copies of the intensity-imaged phase mask pattern. This is a different paradigm from standard
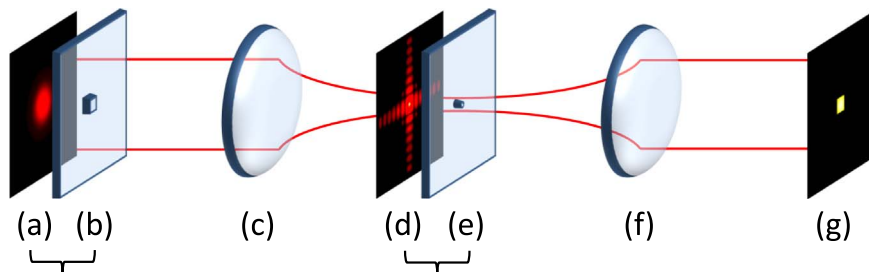

Fig. 1. Standard GPC setup consisting of an input phase mask (b), Fourier lenses (c) & (f) and a PCF (e). The input illumination (a), its Fourier transform, after applying the phase mask (d) and the imaged intensity (g) are also shown. (Not drawn to scale).
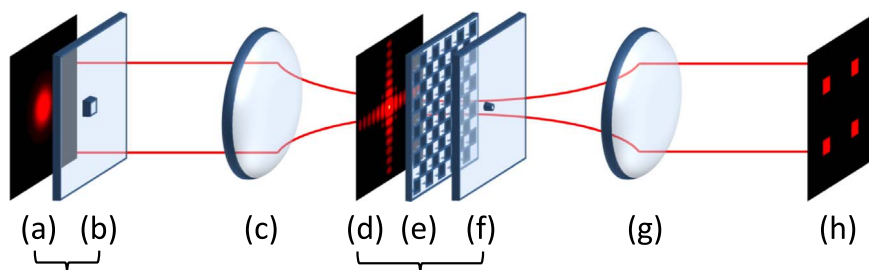

Fig. 2. Holo-GPC setup. Compared to standard GPC, a hologram (e) is placed in addition to the PCF at the Fourier plane of the first lens. For practical implementations, the hologram is typically encoded on an SLM, and the sizes of the input beam, phase mask, PCF and focal lengths have to be adjusted. The second lens (g) optically Fourier transforms the light that is altered by the hologram and PCF to get a distributed output consisting of speckle-free contiguous shapes.

GPC wherein a phase mask utilizes multiple smaller sub-shapes that need not be identical, and hence the corresponding output individual beams can also have different shapes. However, unlike standard GPC, Holo-GPC's output beams are not constrained to an imaging plane, but rather, can be addressed in a 3D holographic manner. Furthermore, a compensating phase mask region [1,9] is not necessary for maintaining the optimal fill factor while changing the number of output beams.

3. Experiments

Our preliminary setup is illustrated in Fig. 3. We used a λ=750 nm laser source (filtered supercontinuum laser from NKT Photonics) and re-purposed a static GPC-LS from [14] with the PCF displaced from the beam path. An 8x magnified image of the GPC-LS's focal plane is used to illuminate a phase-only SLM (Hamamatsu Photonics, pitch=20 μm). The SLM-encoded PCF shifting region has a diameter of 21 pixels or 420 μm which is very close to the theoretical optimal 423.26 μm [9]. The complex field at the SLM plane is optically Fourier transformed with an *f* =300 mm lens, then magnified for sufficient coverage of the CCD camera. The current setup allows qualitative assessment of the output by comparing with the output when using the calibrated glass PCF in the GPC-LS (imaged into the SLM) instead of the SLM-based encoded PCF. There is slightly less contrast when using the SLM as a PCF and this may be due to pixilation errors or the less precise placement of the SLM compared to the glass PCF. However, this lessened contrast did not prevent obtaining definitive results and also shows that the fabricated PCF is not strictly necessary. When both SLM-based and glass PCFs are present, a moderate cancellation of the GPC effect was also observed.

For the holograms, we tested a simple binary checkerboard grating, multiplexed spots distributed in 3D and a spot array generator. The multiplexed spots are based on the lenses and prisms phases encoded on non-overlapping random SLM regions that are assigned to each

spot. For visualization, a blazed grating was used to shift the spot patterns away from the zero-order diffraction. The amplitude profile of the Fourier transformed phase mask is not used in the hologram calculations and uniform illumination was used instead. For a given CGH, different phase masks were used to form different PSF shapes.

4. Results

The output reconstructions from the binary checkerboard grating using different input phase masks are shown in Fig. 4. Some loss in sharpness and fringing can be attributed to the finite SLM window and lens apertures, but the patterns remain recognizable. The same SLM hologram is used even for the arbitrarily shaped phase masks. Although the individual intensities in the array are not uniform, the relative intensity gain from using GPC is clearly observed. Fig. 5 demonstrates 3D addressing with Holo-GPC by using a multi-spot hologram and then imaging the reconstructed output at planes by translating the camera by 215 mm. Despite some noise from the hologram among the individual beams, it is clear that the square mask is focused at different planes and exhibits expected diffraction patterns at the off-focus planes.

In these experiments, we have ensured that there are enough SLM pixels to draw the required circular phase shifting region of the PCF which in turn defines the SRW that has to interfere optimally at the output. As the size of the PCF shifting region is also close to that of the point spread function of the light distribution at the SLM, this also means that there is sufficient SLM-pixel sampling of the readout beam. Although it is preferable to increase the size of the PCF shifting region, i.e. the zero-order at the SLM, also since this decreases its relative peak intensity, further magnifying the read-out beam pushes more higher spatial frequencies out of the SLM's active area and would reduce the sharpness of reconstructed beams. Hence a trade-off in contrast from a well-formed SRW and sharpness from the included higher spatial frequencies should be considered when scaling the SLM read-out light. The ever increasing resolutions of SLM's help in balancing these trade-offs as exemplified in our experiments. Alternatively, at the cost of added complexity, a high fidelity PCF can be installed separately at a conjugate plane or directly deposited as a phase step on the SLM active window and effectively remove this coupled constraint from the SLM as also suggested in the presented setup.

5. Bringing back focusing using matched filtering

When operating a Holo-GPC setup, the focal spots have to be broadened in order to draw well defined shapes on top of the focal spots. As some applications require stronger focusing it would be convenient to be able to switch between shaped and focused spots without changing the lens magnification. One way to achieve this is to use matched filtering [15]. Rectifying, the alternating signs of the Airy-disk-like lobes with matching concentric phase rings emulates having a flat phase plane wave illumination. The concentric rings are easily applied on top of the PCF and hologram encoded on the SLM. We demonstrate matched filtering using spot array holograms, iteratively optimized [16] from an initial Dammann grating [17] to have more uniform spot intensities as the binary transition points [18] are not precisely represented with the discretized SLM pixels. Fig. 6 shows an initial Gaussian beam array, transformed into circular top hats, then transformed into more focused spots using the matched filtering technique. Since the image gets saturated, the result is also presented at a lower camera gain. Narrower and more intense beams are observed. Although this will not outperform a hologram with a broader top-hat or Gaussian read-out beam, the easy switching from shaped beams makes matched filtering a convenient feature in a Holo-GPC setup and may give an extra "jolt" in optical manipulation applications [19], or higher intensities for secondary or non-linear effects in multi-functional setups [6].
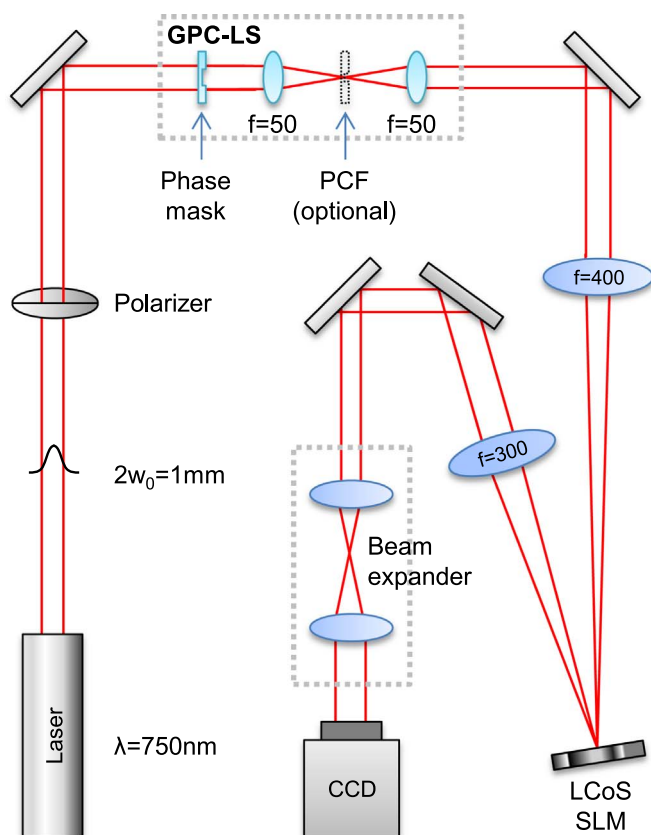

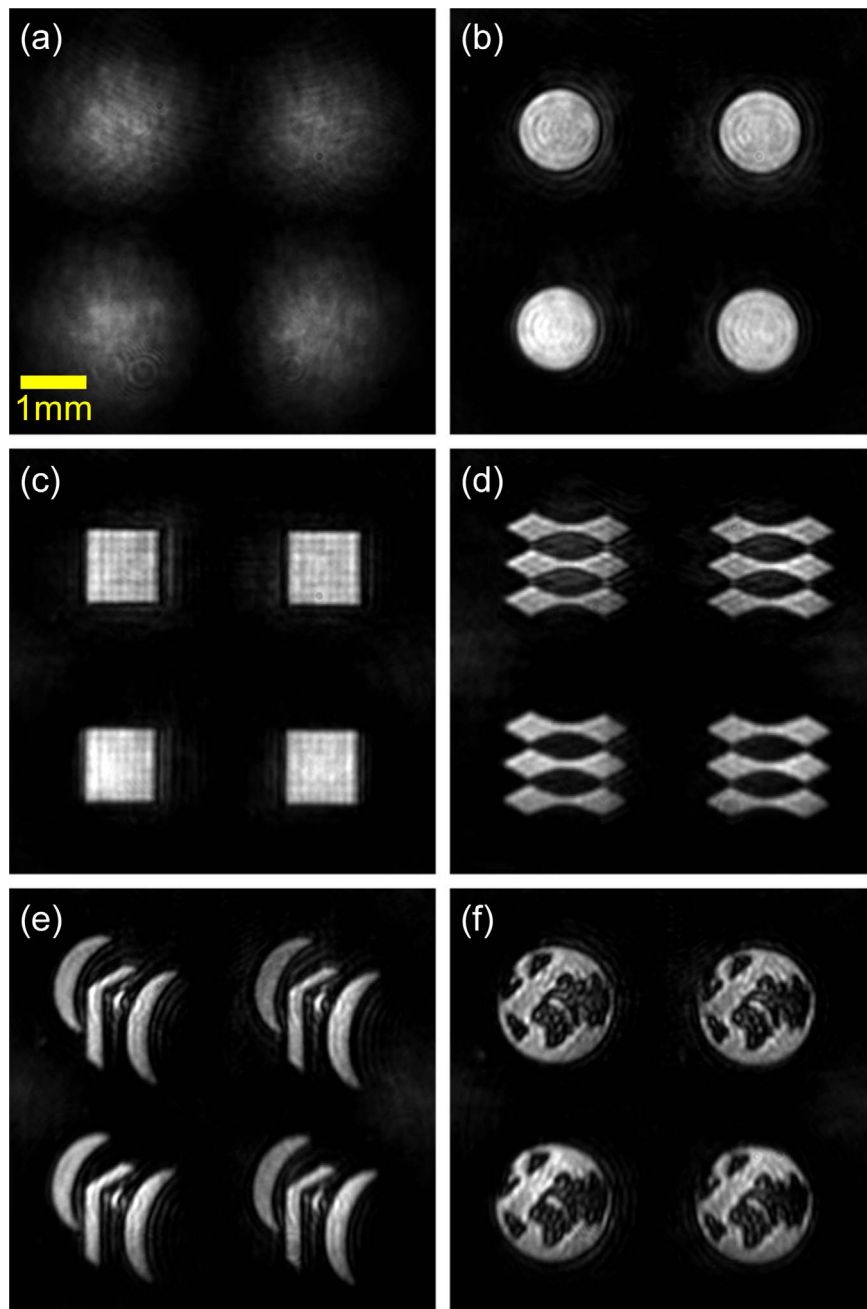**Fig. 3.** Optical setup for Holo-GPC experiments.

Fig. 4. Initial holographic output from a checkerboard grating (a), then with Holo-GPC encoded with different phase masks (b)-(f). The scale bar corresponds to 1 mm at the camera.
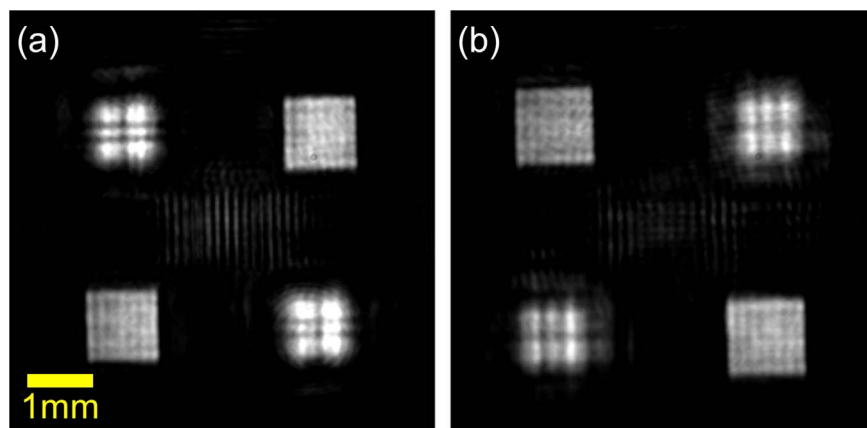

Fig. 5. Holo-GPC addressing beams in 3D. Planes in (a) and (b) are 215 mm apart axially and include both "in focus" and diffracted "out-of-focus" square beam reconstructions.
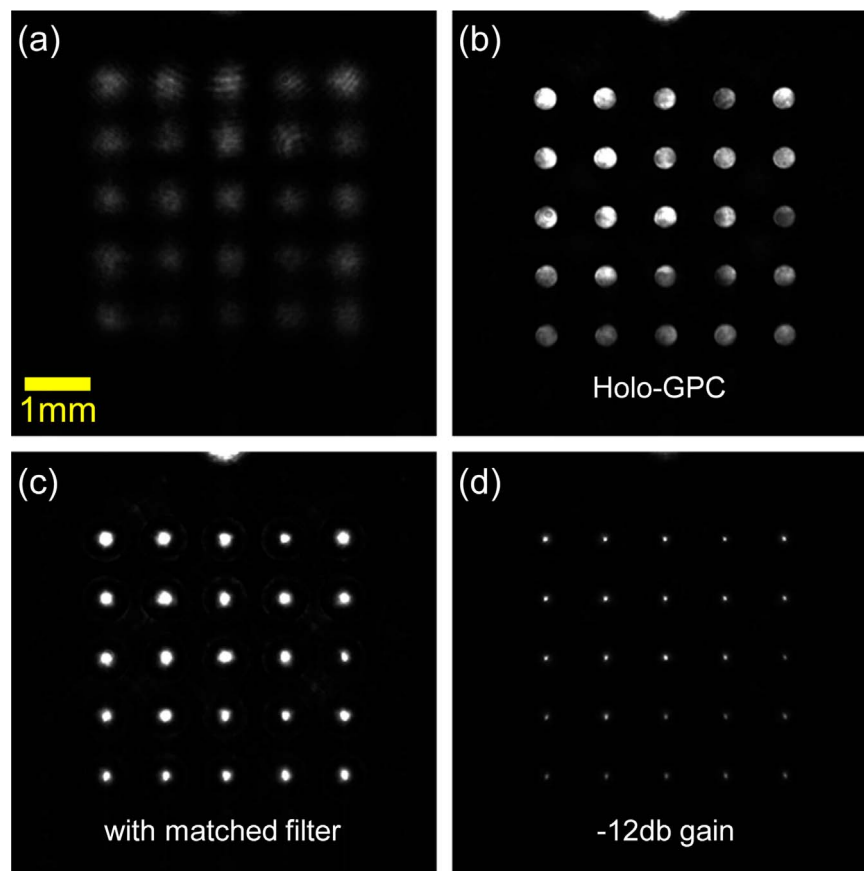
Fig. 6. A 5×5 holographically diffracted Gaussian spot array (a) shaped into circles via Holo-GPC (b), then converted into intense spikes (c) via matched filtering. To reduce the saturation (d), the camera gain had to be 12db lower.

6. Conclusions

We have presented an efficient phase-only light shaping approach that simultaneously controls the distribution of multiple beams and shape these beams individually. Holo-GPC therefore extends the capabilities of either GPC or holography. Holo-GPC is a hybrid of holography that can create extended 2D or 3D beam distributions and GPC that forms noise-free sculpting of the individual beams. Our preliminary experiments show how Holo-GPC is easily implemented with a phase-only SLM and simple binary phase patterns that determine the shape of the beams or PSFs. Instead of being limited to round spots with intensity roll-offs, Holo-GPC makes it possible to have spatially distributed structured beams with well-defined high contrast boundaries. The resulting shaped intensity profiles can provide more precision and contrast in applications such as laser materials processing or for two-photon optogenetics. If necessary, further improvements are possible by using an actual high fidelity PCF, and using more sophisticated hologram calculation algorithms. If the cost and efficiency trade-offs using an extra SLM are acceptable, having a dynamic input phase mask also significantly increases Holo-GPC's versatility. Special purpose lower resolution SLM's [20] can also be utilized for a small set of pre-defined shapes. We have also shown that one can easily switch between laterally shaped beams into more focused spots using matched filtering. This alternate matched filtering modality, further extends the versatility of a Holo-GPC system and makes it easier to adopt in holographic setups that require stronger focusing.

References

[1] E. Papagiakoumou, F. Anselmi, A. Bègue, V. de Sars, J. Glückstad, E.Y. Isacoff, V. Emiliani, Scanless two-photon excitation of channelrhodopsin-2, Nat. Methods 7 (2010) 848–854. http://dx.doi.org/10.1038/nmeth.1505.

[2] E. Papagiakoumou, Optical developments for optogenetics, Biol. Cell 105 (2013) 443–464. http://dx.doi.org/10.1111/boc.201200087.

[3] D. Palima, A.R. Bañas, G. Vizsnyiczai, L. Kelemen, P. Ormos, J. Glückstad, Wave-guided optical waveguides, Opt. Express 20 (2012) 2004–2014 ⟨http://www.ncbi.nlm.nih.gov/pubmed/22330441⟩.

[4] S.W. Hell, J. Wichmann, Breaking the diffraction resolution limit by stimulated emission: stimulated-emission-depletion fluorescence microscopy, Opt. Lett. 19 (1994) 780–782. http://dx.doi.org/10.1364/OL.19.000780.

[5] D. Palima, A.R. Bañas, G. Vizsnyiczai, L. Kelemen, T. Aabo, P. Ormos, J. Glückstad, Optical forces through guided light deflections, Opt. Express 21 (2013) 581–593 ⟨http://www.ncbi.nlm.nih.gov/pubmed/23388951⟩.

[6] M. Villangca, D.Z. Palima, A. Banas, J. Gluckstad, Light-driven micro-tool equipped with a syringe function, Light Sci. Appl. 5 (2016).

[7] F.O. Olsen, K.S. Hansen, J.S. Nielsen, Multibeam fiber laser cutting, J. Laser Appl. 21 (2009) 133–138.

[8] T. Matsuoka, M. Nishi, M. Sakakura, K. Miura, K. Hirao, D. Palima, S. Tauro, A. Bañas, J. Glückstad, Functionalized 2PP structures for the BioPhotonics Workstation, in: D.L. Andrews, E.J. Galvez, J. Glückstad (Eds.), Proc. SPIE, 2011, p. 79500Q. doi:10.1117/12.877189.

[9] A. Bañas, D. Palima, M. Villangca, T. Aabo, J. Glückstad, GPC light shaper for speckle-free one- and two- photon contiguous pattern excitation, Opt. Express 7102 (2014) 5299–5310. http://dx.doi.org/10.1364/OE.22.005299.

[10] H.O. Bartelt, Applications of the tandem component: an element with optimum light efficiency, Appl. Opt. 24 (1985) 3811 ⟨http://www.ncbi.nlm.nih.gov/pubmed/18224124⟩.

[11] H.O. Bartelt, Computer-generated holographic component with optimum light efficiency, Appl. Opt. 23 (1984) 1499 ⟨http://www.ncbi.nlm.nih.gov/pubmed/18224124⟩.

[12] M.A. Go, P.-F. Ng, H. a. Bachor, V.R. Daria, Optimal complex field holographic projection, Opt. Lett. 36 (2011) 3073–3075 ⟨http://www.ncbi.nlm.nih.gov/pubmed/21847164⟩.

[13] M. Villangca, A. Bañas, D. Palima, J. Glückstad, GPC-enhanced read-out of holograms, Opt. Commun. 351 (2015) 121–127. http://dx.doi.org/10.1016/j.optcom.2015.04.057.

[14] A. Bañas, O. Kopylov, M. Villangca, D. Palima, J. Glückstad, GPC light shaper: static and dynamic experimental demonstrations, Opt. Express (2014). http://dx.doi.org/10.1364/OE.22.023759.

[15] A. Bañas, D. Palima, J. Glückstad, Matched-filtering generalized phase contrast using LCoS pico-projectors for beam-forming, Opt. Express 20 (2012) 9705–9712 ⟨http://www.ncbi.nlm.nih.gov/pubmed/24258701⟩.

[16] R.W. Gerchberg, W.O. Saxton, A practical algorithm for the determination of the phase from image and diffraction plane pictures, Opt. (Stuttg.). 35 (1972) 237–246.

[17] H. Dammann, E. Klotz, Coherent Optical Generation and Inspection of Two-dimensional Periodic Structures, Opt. Acta Int. J. Opt. 24 (1977) 505–515. http://dx.doi.org/10.1080/713819570.

[18] C. Zhou, L. Liu, Numerical study of Dammann array illuminators, Appl. Opt. 34 (1995) 5961–5969. http://dx.doi.org/10.1364/AO.34.005961.

[19] H.-U. Ulriksen, J. Thogersen, S. Keiding, I.R. Perch-Nielsen, J.S. Dam, D.Z. Palima, H. Stapelfeldt, J. Gluckstad, Independent trapping, manipulation and characterization by an all-optical biophotonics workstation, J. Eur. Opt. Soc. Rapid Publ. 3 (2008) 8034. http://dx.doi.org/10.2971/jeos.2008.08034.

[20] M. Zenou, M. Reznikov, M. Manevich, J. Varshal, Y. Reznikov, Z. Kotler, Adaptive beam shaper based on a single liquid crystal cell, Opt. Commun. 290 (2013) 115–117. http://dx.doi.org/10.1016/j.optcom.2012.10.018.